Development of a New Videosonde Observation System for In-situ Precipitation Particle Measurements

Kenji Suzuki[1], Kensaku Shimizu[2], Tadayasu Ohigashi[3], Kazuhisa Tsuboki[3], Satoru Oishi[4],
Seiji Kawamura[5], Katsuhiro Nakagawa[5], Kosei Yamaguchi[6], and Eiichi Nakakita[6]

[1]*Yamaguchi University, Yamaguchi, Japan*
[2]*Meisei Electric Co., Ltd., Isezaki, Japan*
[3]*Hydrospheric Atmospheric Research Center, Nagoya University, Nagoya, Japan*
[4]*Research Center for Urban Safety and Security, Kobe University, Kobe, Japan*
[5]*National Institute of Information and Communications Technology, Koganei, Japan*
[6]*Disaster Prevention Research Institute, Kyoto University, Uji, Japan*

Abstract

A new videosonde receiving system consisting of two receiving antennas for a set of videosonde and GPS radiosonde has been developed. The antenna for the videosondes is controlled by a GPS slave method, in which the antenna elevation and azimuth are processed every second using GPS location data obtained from a GPS radiosonde attached to the videosonde. The results of the first experimental flight conducted in Okinawa as part of a synchronized observation campaign of a C-band polarimetric radar and videosondes reveal successful reception of clear images of precipitation particles in clouds.

1. Introduction

Aircraft observation is an effective in-situ method, which provides valuable measurements of microphysical properties within clouds, and has provided substantial information on horizontal cloud structure. However, water, heat, and radiative transfer calculations and numerical models require a knowledge of the microphysical properties of the vertical cloud structure. Although aircraft can make vertical soundings during spiral descents, manned research aircraft are unable to fly in severe weather conditions. Therefore, a new type of radiosonde, namely, the videosonde, has been developed to reveal the vertical distribution of hydrometeors (Takahashi 1990). The videosonde is relatively inexpensive and easy to operate. The main component of the device is a video camera used to record images of precipitation particles. Since the first videosonde soundings at Ponape (Takahashi and Kuhara 1993), several hundred videosondes have been launched into the clouds in climatologically different areas and have contributed to better understanding into cloud microphysics (Takahashi et al. 1995a, 1995b; Takahashi et al. 1999; Keenan et al. 2000; Takahashi et al. 2001; Takahashi and Keenan 2004; Takahashi 2006; Takahashi and Suzuki 2010; Takahashi 2010).

Murakami and Matsuo (1990) also developed the hydrometeor videosonde (HYVIS) in order to clarify microphysical structures in clouds, and the HYVIS has been improved by Orikasa and Murakami (1997) and Orikasa et al. (2005). HYVIS was used in the many previous observational studies (Matsuo et al. 1994; Mizuno et al. 1994; Murakami et al. 2003; Kusunoki et al. 2004, 2005; etc.). The same receiving system can be used for videosondes and HYVIS. These were manufactured at Meisei Electric Co. during the late 1980's, and currently, only three receiving systems are available.

The videosonde is a useful tool for giving important information for remote sensing techniques such as polarimetric radar.

Polarimetric radar can estimate cloud microphysics, such as raindrop size distributions and classification of cloud hydrometeors, and improve the accuracy of quantitative rainfall estimation by using appropriate combination of polarimetric parameters. To investigate the relationship between the polarimetric parameters and hydrometeors, simultaneous observations by videosondes and polarimetric radar are essential. Nakakita et al. (2008, 2009) conducted an in-situ observation campaign with synchronization of videosondes and COBRA, which is a C-band polarimetric radar (Nakagawa et al. 2003) at the National Institute of Information and Communications Technology (NICT), Okinawa Electromagnetic Technology Center. After the launch of a videosonde, the Range Height Indicator (RHI) scans by COBRA were continuously performed every minute, targeting the videosonde in the precipitating cloud. A total of 31 videosondes were launched into precipitating clouds during the campaign observation from 2007 to 2009. Nakakita et al. (2009) revealed the possibility of estimating the state that different types of the precipitation particles were mixed up together, using the polarimetric parameters obtained from COBRA.

However, the videosonde observation has some disadvantages. The receiving antenna must be fixed near the videosonde launching site, and so it is necessary to wait for precipitating clouds to pass over the launching site. In addition, since videosonde sounding requires at least one hour, continuous launches into the same rain system are not possible with a single receiving system. In order to overcome these disadvantages, we have developed a new videosonde receiving system that is characterized by a new tracking technique and a low-cost, lightweight receiving system.

In this paper, we report the development of this new videosonde receiving system and the results of a preliminary experiment conducted as a part of the in-situ observation campaign by COBRA synchronized with videosondes in Okinawa from May 25 to June 9, 2011. While analysis using other data such as those derived from COBRA radar is currently being undertaken, this study focuses on describing the development of a new videosonde observation system and those microphysical features revealed from the first experimental flight of a videosonde.

2. New videosonde observation system

The videosonde consists of a Charge Coupled Device (CCD) camera, a video amplifier, and a transmitter. Images of particles are converted to frequencies between 60 Hz and 1 MHz and are transmitted to the receiving system by means of a 1680-MHz carrier wave (bandwidth: 4 MHz, transmission power: 0.5 W) at the surface before being displayed and recorded on videotapes. The videosonde is launched along with a 400-MHz GPS radiosonde (RS-06G; Meisei Electric Co., Ltd.). Because of the directivity, the 1680-MHz receiving antenna must track a videosonde. Therefore, the old-style antenna was manually rotated toward the launched videosonde before the videosonde disappeared into the clouds.

Once the antenna caught the signal from the videosonde, the automatic tracking started and the antenna was controlled by the signal strength. Once the signal was lost by accident, the antenna could no more continued to receive data from the videosonde. The new videosonde observation system developed in the present study uses a different tracking method. The new videosonde receiving system uses a GPS slave method that automatically controls the antenna elevation and azimuth based on the location information obtained from the RS-06G GPS radiosonde attached to the videosonde. Automatic start of the tracking saves labor and reduces risks in severe conditions such as a strong wind and lightning.

Figure 1a shows a schematic diagram of the new videosonde receiving system. It has two antennas for receiving 1680-MHz and 400-MHz signals for videosondes and GPS radiosondes, respectively. A balloon filled with helium gas and a videosonde with a GPS radiosonde are prepared before the approach of rain clouds. After launch, the 1680-MHz antenna (Fig. 1b) can be controlled automatically by GPS information. The GPS location data are processed every second, and the 1680-MHz antenna for a videosonde is controlled in such a case where the angle of the antenna must change more than 2 degrees per second. Therefore, even if the videosonde goes out of sight, the 1680-MHz signal can be tracked as long as the 400-MHz signal from the GPS radiosonde is received. Moreover, the videosonde can be tracked and images of precipitation particles can be received even far from the launching site. The transmission range is designed with 100 km. Operation of the new low-cost, lightweight receiving system has been simplified. Table 1 shows the specifications of the new videosonde observation system.

The videosonde used in the present study was an improved version of that designed by Takahashi (1990), being lighter and less expensive while providing the same level of performance. Its weight is approximately 1.7 kg, which is 2.2 kg less than that used by Takahashi (1990). A simple version of the videosonde without the measurement of particle electric charge has only a weight of 1.0 kg. We also succeeded in reducing the cost to two thirds of the original. The videosonde has a stroboscopic illumination that provides information on particle size and shape. Because the videosonde can obtain particle images without contact, it can measure particles neither bouncing nor destroyed on a film; this feature is different from a film-capture-type one such as the snow crystal sonde by Magono and Tazawa (1966). Interruption of the infrared beam by particles triggers a strobe, and particle images are then captured by a CCD camera. The minimum performance of the infrared sensor is to completely react to a particle of 0.5 mm or larger in diameter. Dead time by the charge of the strobe has been reduced to 0.2 second. Sampling volume that the CCD camera can capture the image by a strobe is $22 \times 18 \times 30$ mm. The recorded precipitation particles were classified as either raindrops, frozen drops, graupel, ice crystals, or snowflakes based on transparency and shape, as described by Takahashi and Keenan (2004). A videosonde is launched by using balloon of 1.2 kg type with helium gas having approximately 5 kg of buoyancy (Fig. 1c). Profiles of atmospheric pressure, temperature, humidity, and wind are obtained from Meisei RS-06G radiosonde attached to the videosonde. Two transmitters of 1680-MHz and 400-MHz are equipped approximately 30 cm apart inside the payload.

3. Results of the first experimental flight using a new videosonde observation system

During the in-situ observation campaign by COBRA synchronized with videosondes in Okinawa from May 25 to June 9, 2011, we tested the reception of images from a videosonde by the newly developed receiving system. On June 1st, a tropical depression was located near Taiwan, and the Baiu front was over the Okinawa Island. RHI scan by COBRA (128°03′50″N, 26°35′11″E) located 24 km northeast of the videosonde observation site was continuously operated every minute, targeting a launched videosonde. It exhibited typical stratiform radar echoes with a clear bright band (Fig. 2). Precipitation particles were observed up to an altitude of 7.5 km. A videosonde was launched into a steady precipitating cloud at 1850 JST from the NICT Okinawa Electro-
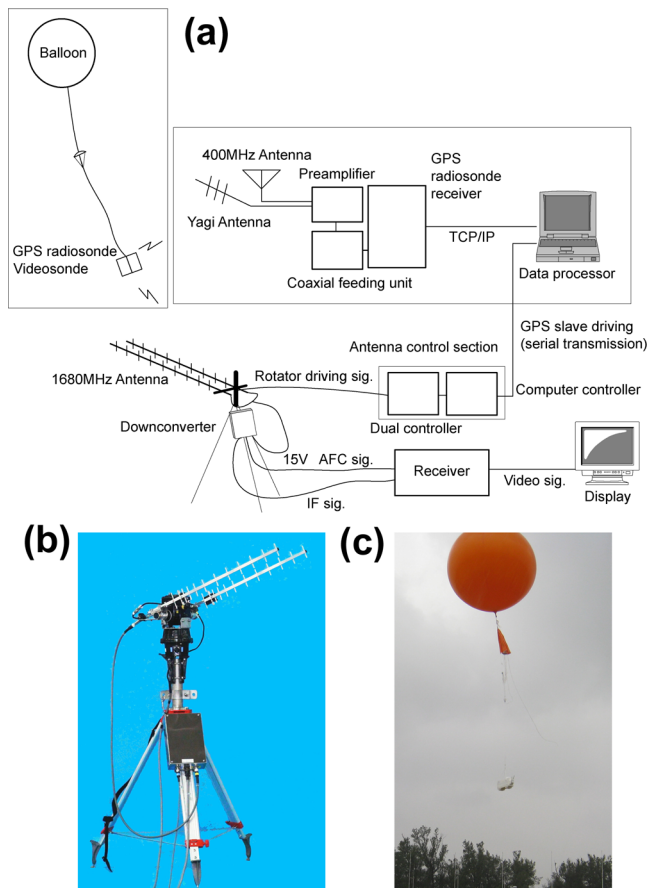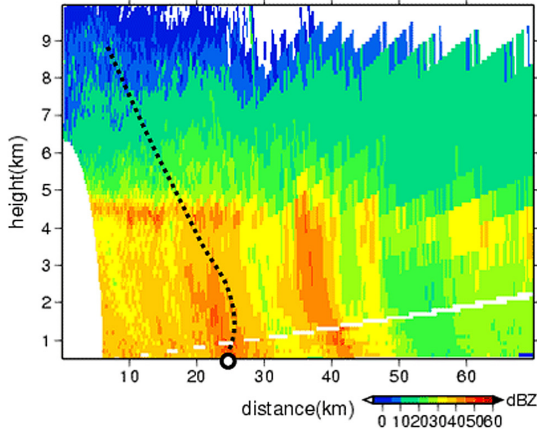

Fig. 1. (a) Schematic diagram of the new videosonde observation system, and photographs of (b) 1680-MHz yagis antenna and (c) launching a videosonde.

Table 1. Specifications of the new videosonde observation system. The details about GPS radiosonde (RS-06G; Meisei Electric Co., Ltd.) is shown in the following URL. http://www.meisei.co.jp/english/products/meteo/rs06g_gps_radiosonde.html

Receiving System	Antenna type	Stucking two yagis antenna
	Frequency	1660~1700 MHz
	Antenna again (min)	14 dBi
	Antenna directivity	H-side: 12 deg, E-side: 29 deg
	Down converter input range	−100~−20 dB
	Down converter output frequency	30 MHz
	Antenna movable range	AZ: 0~440 deg, EL: 0~90 deg
	Antenna tracking speed	AZ: 5 deg/sec, EL: 2 deg/sec
	Center frequency	30 MHz
	Bandwidth	3.0 MHz
	Receiver sensibility (max)	−80 dBm
	Transmission range	100 km
	Output signal	1 Vp-p 75 ohm Video signal
	Antenna control	GPS slave method
	Communication	RS-232C
Videosonde	Video picture	Black and white
	Transmission power	0.5 W
	Video band width	10 Hz to 1 MHz
	Modulation	FM
	Band width	Less than 4 MHz
	Dimensions	$400 \times 140 \times 220$ mm
	Weight	1.7 kg (1.0 kg)

(a) 1844JST, Azimuth=246º

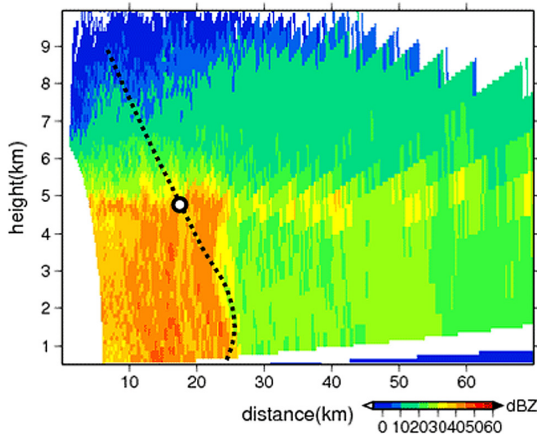## (b) 1910JST, Azimuth=255º

Fig. 2. RHI images detected by COBRA radar at (a) 1844 JST, and (b) 1910 JST on June 1st, 2011. Circles and dot lines indicate locations and trajectories of the videosonde, respectively.
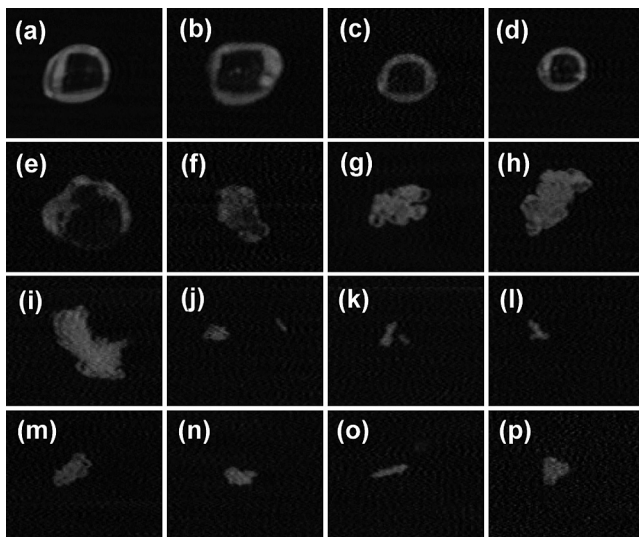

Fig. 3. Precipitation particle images obtained from the videosonde, launched at 1850JST on June 1st, 2011. The width of one frame is 6.5 mm. (a) 3.1 km, 7.7°C, (b) 3.2 km, 7.5°C, (c) 4.3 km, 2.4°C, (d) 2.0 km, 13.0°C, (e) 3.5 km, 5.7°C, (f) 4.7 km, 0.4°C, (g) 4.9 km, −0.7°C, (h) 4.7 km, −0.1°C, (i) 5.1 km, −1.6°C, (j) 5.1 km, −1.8°C, (k) 5.9 km, −5.4°C, (l) 5.8 km, −4.6°C, (m) 5.2 km, −2.2°C, (n) 5.5 km, −3.3°C, (o) 5.7 km, −4.6°C, and (p) 5.3 km, −2.2°C.

magnetic Technology Center (26°29′55″N, 127°50′41″E). Images transmitted from the videosonde were received by old and new receivers. One minute after launching the videosonde, automatic tracking by the GPS slave method was started. Clear images of precipitation particles were captured throughout the cloud. Figure 3 shows precipitation particles transmitted from the videosonde to the new receiving system. The new receiver was confirmed to have provided clear particle images, similar to those provided by the previous receiver.

Figure 4 shows the precipitation particle size-height diagram of the videosonde. The precipitation particles were raindrops below the freezing level and aggregates around the freezing level. Graupel and ice crystals were observed from 5 km through 7.5 km in altitude. Table 2 shows the microphysical features in different temperature ranges. The updraft was supposed to exist around the freezing level because of the high ascent rate of the videosonde
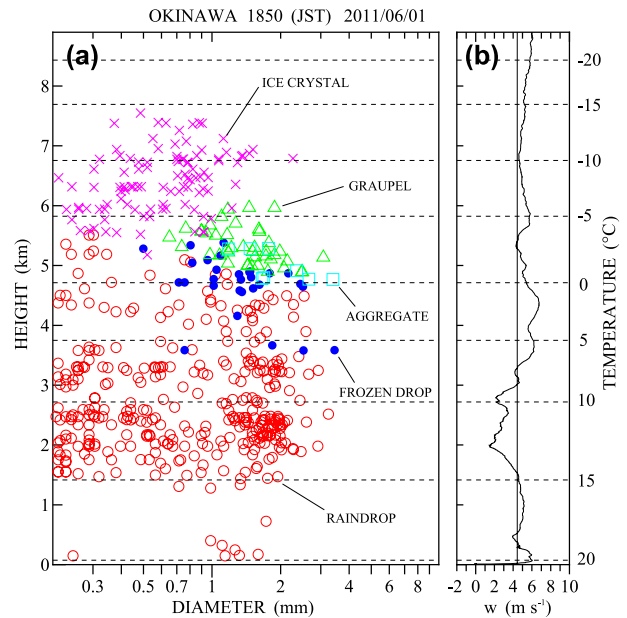

Fig. 4. (a) Precipitation particle size-height diagram of the videosonde ascent at 1850 JST, June 1st, 2011. Open circle (raindrop), solid circle (frozen drop), triangle (graupel), cross (ice crystal), and square (aggregate). (b) Ascent rate (m s^{-1}) of the videosonde. A line indicates the mean ascent rate (4.3 m s^{-1}) averaged below −20°C level.

Table 2. Microphysical features of each particle in the different temperature ranges obtained from the videosonde sounding. Mass and number density were calculated according to Takahashi et al. (1995a) and Takahashi and Keenan (2004).

(Asai 1968), and the existence of supercooled water is suggested there. The fact that the mean diameter of graupel was slightly larger than that of frozen drops suggests that frozen drops uplifted by the updraft were rimed to form graupel (Harimaya 1976). Moreover, the number concentration of ice crystals are less than that of deep stratiform clouds (Takahashi et al. 1995; Takahashi and Keenan 2004) by 1−2 orders of magnitude. The mean diameter of aggregate is small, and the shape is not flake-like but with rounded outlines as shown in Fig. 3g, 3h. It is different from snowflakes consisting of ice crystals observed in deep stratiform anvil clouds. This may be related to the inactive ice crystal formation in the upper level of the shallow stratiform cloud. Aggregates observed in this study were assumed to have formed by the aggregation of small frozen drops and graupel.

We confirmed that the new videosonde observation system, developed in the present study, has equivalent performance to the previous one. Further, videosonde observations will increase our understanding of the microphysical properties within precipitating clouds.

4. Summary

A new videosonde receiving system, which uses a GPS slave tracking method, was developed, and a test flight was conducted as part of the in-situ observation campaign by COBRA synchronized with videosondes in Okinawa. The videosonde was successfully tracked by the new antenna, and precipitation particle images received by the new system were as clear as those received by the previous receiver.

Videosonde is a powerful tool for in-situ measurement within clouds. In the present study, the videosondes developed were low-cost and lightweight, which will enable more videosonde launches to be made. The development of this new videosonde observation system will make various in-situ microphysical measurements possible and provide important information to help clarify the precipitation mechanisms. If multiple receiving sets are available, by using different carrier waves, several videosondes can be launched simultaneously or continuously at a short interval. For example, we can follow the development stages of a single rain system by short-time-step continuous launchings of videosondes. During the campaign, we also launched two videosondes, one at 1673 MHz and the other at 1680 MHz, within 10 minutes using two receiving systems to test the capability of quasi-simultaneous soundings. We obtained clear images from both of the two videosondes. It was clear evidence of no interference between them. In addition, simultaneous videosonde launches at different observation sites would enable direct measurement of three-dimensional microphysical structures in the same cloud system. The new videosonde observation system is capable of determining both spatial and temporal variations of rain systems, and can provide important information regarding cloud microphysics.

Acknowledgements

References

Asai, T., 1968: An analysis of convective activity in the atmosphere using rawinsonde data. *Tenki*, **15**, 109−115.

Harimaya, T., 1976: The embryo and formation of graupel. *J. Meteor. Soc. Japan*, **54**, 42−51.

Keenan, T., P. May, G. Holland, S. Rutledge, R. Carbone, J. Wilson, M. Moncrieff, A. Crook, T. Takahashi, N. Tapper, M. Platt, J. Hacker, S. Sekelsky, K. Saito, and K. Gage, 2000: The maritime continent thunderstorm experiment (MCTEX): Overview and some results. *Bull. Amer. Meteor. Soc.*, **81**, 2433−2455.

Kusunoki, K., M. Murakami, M. Hoshimoto, N. Orikasa, Y. Yamada, H. Mizuno, K. Hamazu, and H. Watanabe, 2004: The characteristics and evolution of orographic snow clouds under weak cold advection. *Mon. Wea. Rev.*, **132**, 174−191.

Kusunoki, K., M. Murakami, N. Orikasa, M. Hoshimoto, Y. Tanaka, Y. Yamada, H. Mizuno, K. Hamazu, and H. Watanabe, 2005: Observations of quasi-stationary and shallow orographic snow clouds: Spatial distributions of supercooled liquid water and snow particles. *Mon. Wea. Rev.*, **133**, 743−751.

Magono, C., and S. Tazawa, 1966: Design of a "snow crystal sonde." *J. Atmos. Sci.*, **23**, 618−625.

Matsuo, T., H. Mizuno, M. Murakami, and Y. Yoshida, 1994: Requisites of graupel formation in snow clouds over the Sea of Japan. *Atmos. Res.*, **32**, 55−74.

Mizuno, H., T. Matsuo, M. Murakami, and Y. Yamada, 1994: Microstructure of cirrus clouds observed by HYVIS. *Atmos. Res.*, **32**, 115−124.

Murakami, M., and T. Matsuo, 1990: Development of the hydrometeor videosonde. *J. Atmos. Ocean. Tech.*, **7**, 613−620.

Murakami, M., Y. Yamada, T. Matsuo, K. Iwanami, J. D. Marwitz, and G. Gordon, 2003: The precipitation process in convective cells embedded in deep snow bands over the Sea of Japan. *J. Meteor. Soc. Japan*, **81**, 515−531.

Nakagawa, K., H. Hanado, S. Satoh, N. Takahashi, T. Iguchi, and K. Fukutani, 2003: Development of a new C-band bistatic polarimetric radar and observation of typhoon events. *Proc. 31st Conf. on Radar Meteor.*, *Seattle, Amer. Meteor. Soc.*, 863−866.

Nakakita, E., K. Yamaguchi, Y. Sumida, H. Takehata, K. Suzuki, K. Nakagawa, S. Oishi, Y. Shusse, and K. Tsuboki, 2008: Classification of hydrometeors using a C-band polarimetric radar and validation by in-situ campaign observation synchronized with video-sonde. *Annuals of Disas. Prev. Res. Inst.*, *Kyoto Univ.*, **51**, 519−533.

Nakakita, E., K. Yamaguchi, Y. Sumida, H. Takehata, K. Suzuki, K. Nakagawa, S. Oishi, Y. Shusse, K. Tsuboki, and T. Ohigashi, 2009: Development of hydrometeor classification system using polarimetric radar measurements synchronized with the video-sonde observation. *Annual Journal of Hydraulic Engineering, JSCE*, **53**, 361−366.

Orikasa, N., and M. Murakami, 1997: A new version of hydrometeor videosonde for cirrus cloud observations. *J. Meteor. Soc. Japan*, **75**, 1033−1039.

Orikasa, N., M. Murakami, M. Hoshimoto, and Y. Yamada, 2005: Re-evaluation of the collection efficiency of the hydrometeor videosonde for dry snow particles. *J. Meteor. Soc. Japan*, **83**, 439−448.

Takahashi, T., 1990: Near absence of lightning in tropical rainfall producing Micronesian thunderstorms. *Geophys. Res. Lett.*, **17**, 2381−2384.

Takahashi, T., 2006: Precipitation mechanisms in East Asian monsoon: Videosonde study. *J. Geophys. Res.*, **111**, D09202, doi:10.1029/2005 JD006268.

Takahashi, T., 2010: The videosonde system and its use in the study of East Asian monsoon rain. *Bull. Amer. Meteor. Soc.*, doi:10.1175/2010 BAMS2777.1.

Takahashi, T., and K. Kuhara, 1993: Precipitation mechanisms of cumulonimbus clouds at Pohnpei, Micronesia. *J. Meteor. Soc. Japan*, **71**, 21−31.

Takahashi, T., and T. D. Keenan, 2004: Hydrometeor mass, number, and space charge distribution in a "Hector" squall line. *J. Geophys. Res.*, **109**, D16208, doi:10.1029/2004JD004667.

Takahashi, T., and K. Suzuki, 2010: Development of negative dipoles in a stratiform cloud layer in a Okinawa "Baiu" MCS system. *Atmos. Res.*, doi:10.1016/j.atmosres.2010.07.013.

Takahashi, T., K. Suzuki, M. Orita, M. Tokuno, and R. de la Mar, 1995a: Videosonde observations of precipitation processes in equatorial cloud clusters. *J. Meteor. Soc. Japan*, **73**, 509−534.

Takahashi, T., K. Suzuki, C. Wang, and C. Guo, 1995b: Precipitation mechanisms of cloud systems developed in a semi-arid area of Pingliang, China: Videosonde observations. *J. Meteor. Soc. Japan*, **73**, 1191−1211.

Takahashi, T., T. Tajiri, and Y. Sonoi, 1999: Charges on graupel and snow crystals and the electrical structure of winter thunderstorms. *J. Atmos. Sci.*, **56**, 1561−1578.

Takahashi, T., N. Yamaguchi, and T. Kawano, 2001: Videosonde observation of torrential rain during Baiu season. *Atmos. Res.*, **58**, 205−228.